 doi:10.20944/preprints202101.0583.v1

Type of the Paper (Article, Review, Communication, etc.)

Physico-chemical properties of a hybrid biomaterial (pva/chitosan) reinforced with conductive fillers

Olarte-Paredes A.[1]*, Salgado-Delgado J.N.[1], Rubio-Rosas E.[2], Salgado-Delgado A.M.[1], Hernández-Cocoletzi H.[3], Salgado-Delgado R.[1], Moreno-Carpintero E.[1] Castaño V.M. [4*]

[1] Affiliation 1; e-mail@e-mail.com
[2] Affiliation 2; e-mail@e-mail.com
* Correspondence: e-mail@e-mail.com; Tel.: (optional; include country code; if there are multiple corresponding authors, add author initials)
[1] Tecnológico Nacional de México/ IT de Zacatepec, Calzada Tecnológico, No. 27, C.P. 62780, Zacatepec de Hidalgo, Morelos.
[2] Centro Universitario de Vinculación y Transferencia de Tecnología BUAP, Prolongación de la 24 Sur y Av. San Claudio Ciudad Universitaria, Col, Jardines de San Manuel, 72000 Puebla, Pue.
[3] Facultad de Ingeniería Química, Benemérita Universidad Autónoma de Puebla, Av. San Claudio y 18 sur S/N edificio FIQ7 CU, San Manuel Puebla, Pue. C. P. 72570, México.
[4] Centro de Física Aplicada y Tecnología Avanzada, Universidad Nacional Autónoma de México, Boulevard Juriquilla 3001,
Querétaro 76230, México.
* *Authors for correspondence: alfredo.op@zacatepec.tecnm.mx; vmcastano@unam.mx*

Abstract: A novel hybrid material based on Polyvinyl alcohol-Chitosan (PVA-Cs) was made, reinforced with conductive polymer fillers such as polypyrrole (PPy), Poly(3,4-ethylenedioxythiophene)-poly(styrenesulfonate) (PEDOT:PSS), carbon black (CB) and multi-wall carbon nanotubes (MW CNT). Our proposal is to use these fillers, which have not been studied in this context before, for obtaining composite materials, and to characterize them for the development of applications in microelectronics. FTIR analysis made evident the different functional groups present in the matrix and the fillers used. The use of quaternary mixtures (4 fillers) increased the contact angle, which increased the degree of hydrophobicity of the biocomposite. The Nyquist diagram of the analyzed samples showed a decrease in resistance and energy diffusion; the latter due to the transfer of electrons caused by the conductive polymers CB and the MWCNT. In the mechanical tension tests, Young's modulus values of 18.386 MPa were obtained, in contrast with the material matrix of PVA-Cs, which showed values of 11.628 MPa. Furthermore, morphological analysis by SEM showed that the materials obtained were homogeneous, with no phase formation. The materials obtained showed higher electrical conductivity in the presence of the OH and NH2 groups, which could have possible applications in biopolymer electrodes.

Keywords: : electrical conductivity, young module, conductive filled, hydrophobic

1. Introduction

There has been an increasing interest in recent years in the development of films based on conductive polymers due to the inherent properties of these materials [1-3]. Polyvinyl alcohol (PVA) is a material with good structural properties but poor mechanical properties. That is why it is frequently reinforced with chitosan (Cs), which, in addition to improving the mechanical properties of the material, has amino (-NH2) groups, which makes its charge more positive [3-9]. Recent discoveries associated with conductive polymers have generated great interest recently. One of the most outstanding polymers is the derivative of Poly (3,4-ethylenedioxythiophene) -poly (styrenesulfonate) (PEDOT:PSS); its excellent thermal and electrochemical stability makes it a versatile polymer that can be

Preprints (www.preprints.org) | NOT PEER-REVIEWED | Posted: 28 January 2021 doi:10.20944/preprints202101.0583.v1

used in supercapacitors, solar cells and sensors [10-17]. Besides PEDOT:PSS, there are other conductive polymers of great importance, such as polypyrrole (PPy), which has been widely studied due to its good mechanical and electrical properties and has been used as a coating for corrosion protection [15-16]. Multi-wall carbon nanotubes (MWCNT), which have very good mechanical properties compared to conventional materials, have been used recently in the manufacture of composite materials due to their low cost [19-20]. Carbon black (CB), another conductive polymer, has properties that change the mechanical, electrical, thermal, and optical characteristics of the materials over which it is dispersed; in addition, these materials benefit from the unique properties of CB, acquiring UV protection, electrical conductivity, opacity and mechanical reinforcement [21-22]. The present work aims to obtain and characterize composite films (not reported) based on a matrix of Polyvinyl alcohol-Chitosan (PVA-Chi) reinforced with fillers of conductive polymers such as polypyrrole (PPy), poly(3,4 ethylenedioxythiophene) or PEDOT, carbon black (CB) and multi-wall carbon nanotubes (MWCNT). The hypothesis is based on the compatibility of the PVA-Cs matrix with the conductive fillers and the synergetic properties that could arise from the interaction between them.

2. Materials and Methods

2.1 Materials

Polyvinyl Alcohol (PVA), ALDRICH, CAS:9002-89-5, average Mw 8500-124000, 87-89% hydrolyzed. Chitosan (Cs), ALDRICH, CAS: 9012-89-5, medium molecular weight. Polypyrrole (PPy), ALDRICH, CAS:30604-81-0, conductivity 10-50 S/cm. Poly(3,4-ethylenedioxythiophene)-poly(styrenesulfonate) (PEDOT:PSS), ALDRICH, CAS:155090-83-8, 3.0-4.0% of H2O, high degree of conductivity. Multi-wall carbon nanotubes (MWCNT), ALDRICH, CAS:308068-56-6, >90% carbon-based D x L 110 -170 nm x 5.9 μm. Carbon black (CB), MEYER, CAS:1333-86-41 with a superficial area of 85 m2/g and 5% moisture. Acetic acid, ALDRICH, CAS:64-19-7.

2.1 Methods

Preparation of the PVA-Cs matrix solution: Two grams of PVA were mixed with 20 mL of distilled water. The solution was kept under magnetic stirring at a temperature of 75 °C for 25 min until homogenization; 3 mL of Cs solution were then added to this solution. The Cs solution was prepared by mixing 3 g of Cs with a previously prepared solution of 100 mL of acetic acid and distilled water (2% v/v) that was subjected to sonication (ultrasonic homogenization) for 20 h.

PPy filler dispersion: To achieve a good dispersion of PPy particles in the matrix, PPy was added in three concentrations (0.1, 0.2 and 0.3g) to 3 mL of concentrated acetic acid and sonicated for 4 h (ultrasonic homogenization). After sonication, it was incorporated into the PVA-Cs solution by magnetic stirring for 10 min at room temperature.

CB filler dispersion: Carbon black was added in 2 concentrations (0.1 and 0.2 g), sonicating for 3 h to disperse the particles in the PVA-Cs solution.

PEDOT:PSS and MWCNT dispersion: The PEDOT:PSS and MWCNT fillers were added in two concentrations (0.1g and 0.2g in both cases) and incorporated into the PVA-Cs solution by magnetic stirring at a temperature of 40 °C. In addition to these conductive polymers, 0.5 mL of Glycerol was also added to all the samples to act as a plasticizer. The films composed of PVA-Cs with PPy and the fillers (PEDOT:PSS/MWCNT/CB) were made by casting process on a 6 cm diameter petri dish. The samples were allowed to dry at room temperature for 72 h. Table 1 shows the working matrix used for obtaining the composite films.

Preprints (www.preprints.org) | NOT PEER-REVIEWED | Posted: 28 January 2021 doi:10.20944/preprints202101.0583.v1

Table 1. Working Matrix

Sample	PVA-Cs (mL)	PPy (g)	PEDOT:PSS (g)	MWCNT (g)	CB (g)
B1	28	-	-	-	-
B2	28	0.1	-	-	-
B3	28	0.2	-	-	-
B4	28	0.3	-	-	-
B5	28	-	0.1	-	-
B6	28	-	0.2	-	-
B7	28	-	-	0.1	-
B8	28	-	-	0.2	-
B9	28	-	-	-	0.1
B10	28	-	-	-	0.2
B11	28	0.1	0.1	0.1	0.1
B12	28	0.1	0.2	0.2	0.2
B13	28	0.2	0.1	0.1	0.1
B14	28	0.2	0.2	0.2	0.2
B15	28	0.3	0.1	0.1	0.1
B16	28	0.3	0.2	0.2	0.2

2.2 Characterization

Mechanical Evaluation The tensile strength of the materials was evaluated using an INSTRON universal mechanical test machine, model 3340, according to the ASTM D-882 tensile standard for plastic films, at a speed of 30 m/s [23].

Contact angle was analyzed using a goniometer by placing 1 μL of distilled water on the surface of the film (solid-liquid interface) at a temperature of 23 °C. Photographs of the microdrop were taken with 3 s of exposure time. The photographs, which were taken in triplicate, were processed in the matlab image editor to measure the angle formed by the drop of water on the surface.

Fourier-transform infrared spectroscopy (FTIR) The FTIR analysis was performed using a FTIR Spectrophotometer (Perkin Elmer's Spectrum Two). The wave number range used in the analysis was 400-4000 cm-1 in ATR mode. This analysis allows the identification of functional groups in organic materials, as well as any vibrational changes caused by the interaction between them.

Surface Analysis by Scanning Electron Microscopy (SEM) The surface analysis was performed by scanning electron microscopy (SEM) using a JEOL microscope (JSM 6010A) in SEI mode and 1.5 kV without metal coating.

 doi:10.20944/preprints202101.0583.v1

3. Results and Discussion

3.1. Mechanical Analysis of Tension

Table 2 shows the results of the mechanical stress-strain tests. PVA and chitosan (Cs) were subjected to mechanical tests separately. The Cs results are not shown because the films showed fragility when manipulated to perform the test. The PVA samples showed a tensile strength of 10.16 MPa with a deformation of 341.44 mm/mm. In the PVA-Cs mixture, the presence of Cs caused an increase in tensile strength from the 10.16 MPa of PVA alone to 18.84 MPa for the PVA-Cs mixture. With respect to deformation, the presence of Cs in the mixture reduced the percentage of deformation from 341.44 mm/mm for PVA alone to 281.93 mm/mm for the PVA-Cs mixture . This could be due to an increase in the formation of hydrogen bridges between PVA chains and Cs, as has been reported by Agil Abraham, Soloman P. and Rejini V (2016).

The presence of the PPy filler in the PVA-Cs samples increased the mechanical resistance of the composite films, achieving an increase of up to 23.56 MPa in the PVA-CS/PPy0.3 sample. Although PPy has brittle properties, this did not detract from its contribution to mechanical strength but it did render the matrix more susceptible to deformation, reducing its elasticity elasticity from 281.93 mm/mm (PVA-Cs) to 254.58 mm/mm (PVA-CS/PPy0.3). The PEDOT:PSS filler increased the ductility of the materials, while the use of MWCNT improved their mechanical resistance; using a concentration of 0.2 g of each (PVA-Cs/PEDOT:PSS0.2 and PVA-Cs/MWCNT0.2) increased the percentage of deformation and the mechanical resistance of the materials. This did not happen with concentrations of 0.1g (PVA-Cs/PEDOT:PSS0.1 and PVA-Cs/MWCNT0.1) since there was a percolation concentration at precisely 0.2 g, beyond which the mentioned properties increased. The same results have been reported by Villemin E. and Guo X. (2018) [10,17]. It is important to note that the sample representing the B15 quaternary mixture containing 0.3 g of PPy and 0.1 g of the PEDOT:PSS, CB and MWCNT fillers showed high deformation and mechanical resistance values. The presence of PPy significantly contributed to increasing the percentage of deformation, while the interaction of the fillers, used in concentrations of 0.1%, gave greater mechanical resistance to the materials. The PVA-CS/PPy0.3/PEDOT:PSS0.1/MWCNT0.1/CB0.1 sample required a stress of 40.332 MPa for a deformation of 355.252%; thus, it is possible to say that, at these concentrations, the studied fillers improved the resistance to breakage of the material. The Young's modulus of the materials obtained was determined based on the results of the stress and strain tests. The sample of PVA alone had a Young's modulus of 8.083 MPa; when adding Cs to the PVA material, the Young's modulus increased to 10.806 MPa. The molecular structure of Cs gives it physicochemical characteristics that improve the mechanical properties of PVA. This agrees with the results of tensile strength, since Cs was associated with an increase in the mechanical resistance of the material and a decrease in the percentage of deformation. Table 2 shows the results of Tukey' analysis on the Young's modulus of the samples, with a significance level of 0.05.

Increasing the percentage of any of the fillers caused an increase in the Young's modulus of the material, which also agrees with the behavior of tensile strength. The PVA-CS/PPy0.3 film showed better mechanical resistance properties, rigidity, and toughness, with a Young's modulus of 19.67 M Pa, almost double compared to the 10.80 MPa of the PVA-Cs film. These results indicated that there was a positive interaction between PPy and the PVA-Cs material, turning it into a material with potential structural applications. The PVA-CS/PPy0.3/PEDOT:PSS0.1 //MWCNT0.1/CB0.1 material, which contained the four fillers (0.3 g of PPy and 0.1 g each of MWCNT, CB and PEDOT:PSS) had a Young's modulus of 17.579 MPa, slightly less than the value for the PVA-CS/PPy0.3 material, which was 19.67 MPa. This may be since although PPy provided mechanical resistance to the materials, CB and MWCNT particles were dispersed using an ultrasonic bath, which could have affected the molecular structure of the materials.

Preprints (www.preprints.org) | NOT PEER-REVIEWED | Posted: 28 January 2021 doi:10.20944/preprints202101.0583.v1

3.2 Contact angle

Figure 1 shows the contact angle average results for each of the samples. As the results show, the films had a hydrophilic character, which means that their contact angle was less than 90°. In the samples with a single filler (PVA-CS/PPy0.1 to PVA-Cs/PEDOT:PSS0.2 sample´s), either PPy or PEDOT:PSS, the contact angle did not exceed 55°, which indicated that

Sample	Stress (MPa)	Strain (mm/mm)	Young Modulus (MPa)	Young Module Standard Deviation	Young Module Standard Error of Mean
B1	18.84	281.93	10.80667	0.11218	0.06477
B2	20.88	239.98	12.728	0.66916	0.38634
B3	20.55	230.49	18.10667	0.95978	0.55413
B4	23.56	254.58	19.67467	0.35194	0.20319
B5	17.13	279.4	9.38567	1.12666	0.65048
B6	20.59	298.37	12.05367	0.39865	0.23016
B7	15.42	327.71	6.677	0.22598	0.13047
B8	19.11	339.98	8.50333	0.39415	0.22756
B9	20.06	302.91	11.68667	0.81716	0.47179
B10	19.54	214.76	14.40767	1.54626	0.89273
B11	14.57	238.27	12.808	1.17067	0.67589
B12	18.15	314.46	10.74567	0.64616	0.37306
B13	9.91	244.15	7.99667	0.53993	0.31173
B14	11.78	186.86	12.17133	1.12618	0.6502
B15	40.33	355.25	17.579	0.47188	0.27244
B16	21.94	318.6	12.444	0.24258	0.14005

Table. 4 Statical analysis of Mechanical Properties

these samples were even more hydrophilic. The use of allotropic carbon fillers (MWCNT or CB) increased the contact angle of the materials from 60° to 62°, which made samples PVA-Cs/MWCNT0.1 to PVA-Cs/CB0.2 more hydrophobic. This may be due to the sp2 hybridization structure of these fillers. However, the quaternary mixture samples B11 to b16 (which contained the 4 fillers) had the highest contact angles, ranging from 64° to 69°. This may be caused by the interaction between the allotropic carbon fillers, which increased hydrophobicity, and the other fillers. It is important to note that the polymer matrix materials B10 and B17 had different concentrations of PVA-Cs (28 and 25 mL respectively). The PVA-Cs sample had a contact angle of 63°, while the B17 sample had a contact angle of 71°; the latter was the most hydrophobic of the samples, which suggested that decreasing the volume could lead to an increase in the hydrophobicity of the materials and vice versa.

Preprints (www.preprints.org) | NOT PEER-REVIEWED | Posted: 28 January 2021 doi:10.20944/preprints202101.0583.v1

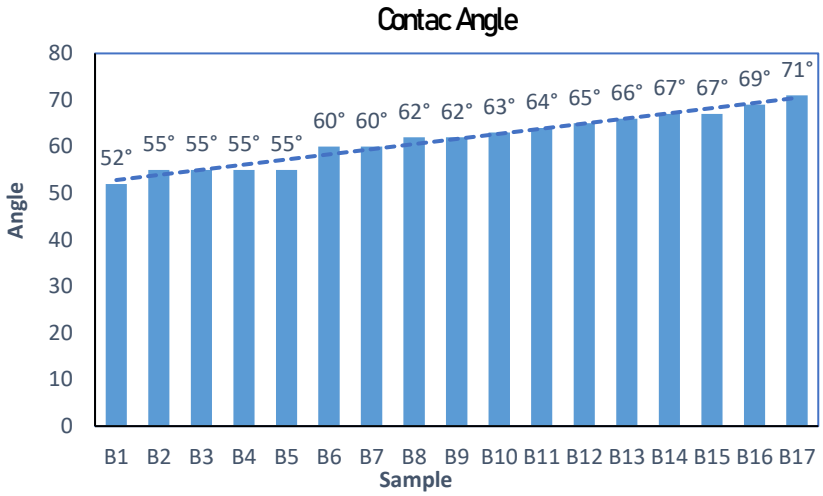

Figure 1. Result of average Contact angle

3.3 Surface Analysis by Scanning Electron Microscopy (SEM)

Figure 2 shows the SEM micrographs, in cross section, of the PVA (A) and PVA-Cs (B) films. Adding Cs to PVA made the material homogeneous and uniform, in addition to the fact that no phase separation can be observed between PVA and Cs. These results suggest that the PVA-Cs material has synergistic properties.

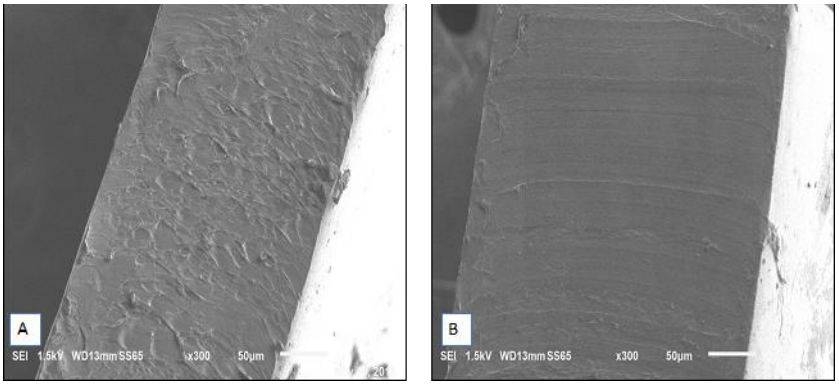

Figure 2. SEM micrographs (300 X) of samples A) PVA, B) PVA-Cs.

Figure 3 shows the SEM micrographs of the composite materials of PVA-Cs mixed with conductive polymers (PPy, CB, MWCNT and PEDOT:PSS). It can be seen that A), C) and D) maintained homogeneity and uniformity, there is good adhesion between the PVA-Cs materials. In the image of the PVA-Cs / CB sample (B) small particles are observed, which may be due to carbon black, which due to their characteristics form dispersed aggregates that are clearly observed in the matrix.

Preprints (www.preprints.org) | NOT PEER-REVIEWED | Posted: 28 January 2021 doi:10.20944/preprints202101.0583.v1

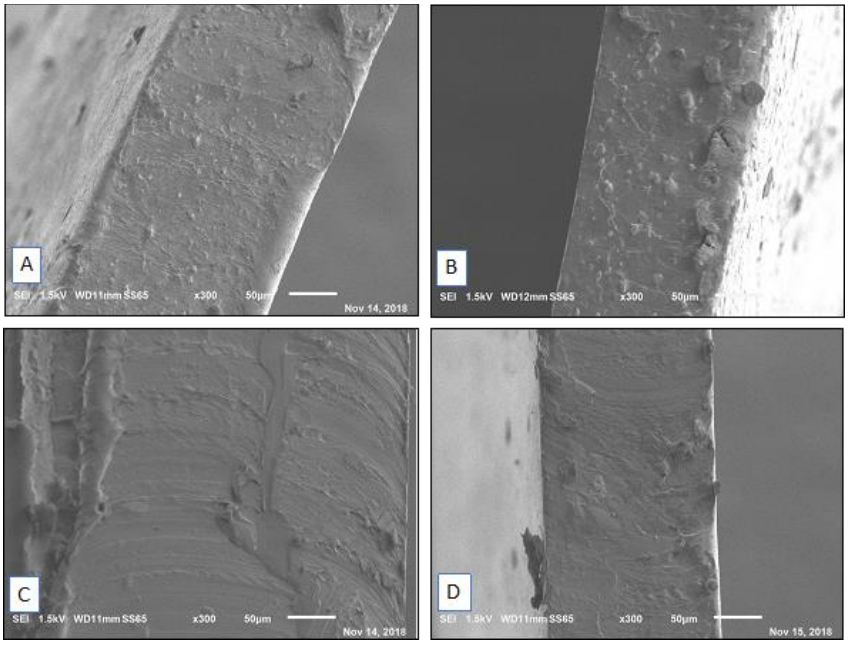

Figure 3. Micrographs (300 X). A) PPy 0.2 g; B) CB 0.2 g; C) PEDOT:PSS 0.2 g; D) MWCNT 0.2 g.

Figure 4 shows SEM micrographs of the composite materials containing the four fillers under study in the PVA-Cs matrix quaternary samples (PVA-CS/PPy/PEDOT:PSS//MWCNT/CB0). As can be seen, the conductive polymers were well dispersed throughout the matrix. Some of the micrographs show small particles, probably of carbon black that was not completely dispersed and which formed aggregates instead. As can be seen in B), C) and D), uniform and homogeneous films were generated, with good adhesion between the materials. Micrographs E) and F) show the formation of small protuberances.

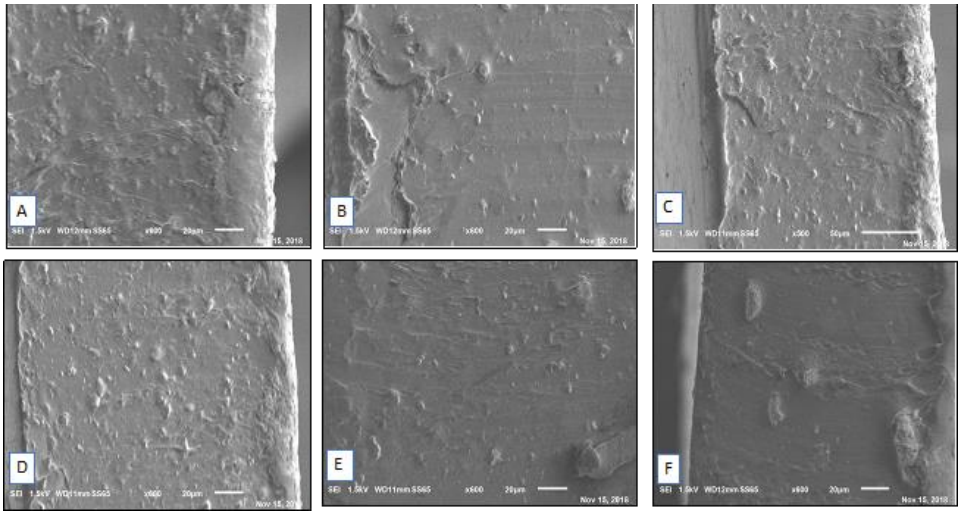

Figure 4. SEM micrographs (600 X). A) PVA-CS/PPy0.3/PEDOT:PSS0.2/MWCNT0.2; B) PVA-CS/PPy0.3/PEDOT:PSS0.1 //MWCNT0.1/CB0.1; C) PVA-CS/PPy0.2/PEDOT:PSS0.2/MWCNT0.2; D)PVA-CS/PPy0.2/PEDOT:PSS0.1//MWCNT0.1/CB0.1;E)PVA-CS/PPy0.1/PEDOT:PSS0.2/MWCNT0.2;F)PVA- CS/PPy0.1/PEDOT:PSS0.1//MWCNT0.1/CB0.1

3.4 Fourier Transform Infrared Spectroscopy (FTIR-ATR)

Figure 5 shows the FTIR spectrum of the PVA-Cs sample, which represents the film containing only the polymer matrix PVA-Cs. The spectrum showed the following signals: in the region of 3500 cm-1, a stretching vibration of the NH bond; at 3100-3300 cm-1, a stretching vibration of the hydroxyl group -OH; at 2900 cm -1, a stretching of the C-H bond; at 1790 cm-1, a stretching band of C=O; at 1600 cm-1, a bending vibration of the –

Preprints (www.preprints.org) | NOT PEER-REVIEWED | Posted: 28 January 2021 doi:10.20944/preprints202101.0583.v1

OH bond due to the formation of hydrogen bridges as a result of the adsorption of water; at 1050 cm-1, a stretching vibration of the C-O bond in the C-O-C and C-OH groups (these functional groups are present in both PVA and Cs). In samples PVA-CS/PPy0.3, PVA-CS/PPy0.2 and PVA-CS/PPy0.1 , in which PPy (0.3, 0.2 and 0.1g respectively) was added to the PVA-Cs matrix, the FTIR spectra showed a decrease in the signal between 3100 and 3300 cm-1, which corresponded to the stretching of the O-H groups. The stretching vibration of the N-H bond in Cs and PPy is more clearly observed at 3500 cm -1. A sharp signal can also be observed at 1600 cm-1, corresponding to the stretching of the C=C bond in PPy. The signal at 1700 cm-1 corresponds to the stretching of the C=O bond in Cs.

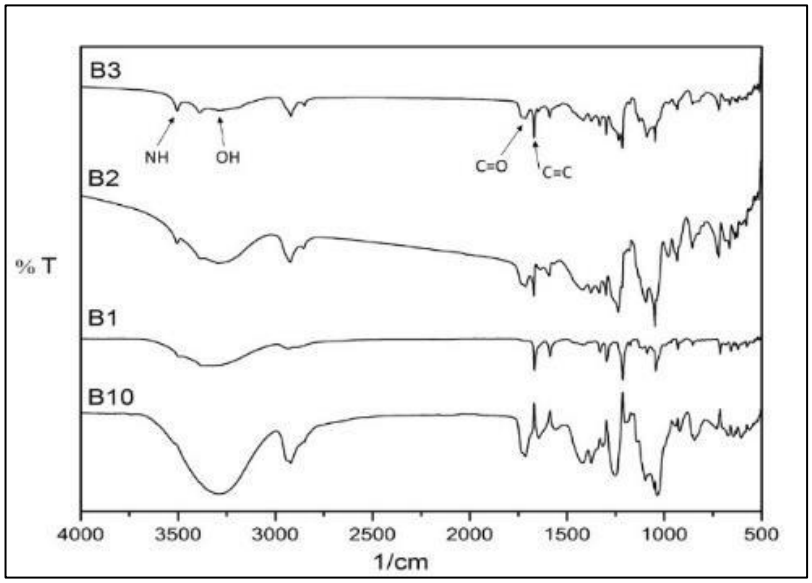

Figure 5. FTIR analysis of the samples PVA-Cs, PVA-CS/PPy0.3, PVA-CS/PPy0.2, PVA-CS/PPy0.1.

Figure 6 shows the FTIR spectrum of samples PVA-Cs/PEDOT:PSS0.2 to PVA-Cs/CB0.2. These images show the samples with PVA-Cs matrix containing a single filler of either PEDOT:PSS, MWNTC or CB. As can be seen, the spectra are very similar, with no great differences in vibration signals between the mentioned fillers. Figure 7 shows the FTIR spectra of samples B10 and B17, which contained only the polymer matrix, and of the samples B11PVA-CS/PPy0.3/PEDOT:PSS0.2/MWCNT0.2, B12PVA-CS/PPy0.3/PEDOT:PSS0.1 //MWCNT0.1/CB0.1, B13PVA-CS/PPy0.2/PEDOT:PSS0.2/MWCNT0.2, B14PVA-CS/PPy0.2/PEDOT:PSS0.1//MWCNT0.1/CB0.1 and B15PVA-CS/PPy0.1/PEDOT:PSS0.2/ MWCNT0.2 , which contained also the four fillers under study (PPy, PEDOT: PSS, MWCNT and CB). The samples that contained the four fillers showed vibration signals at 3100-3500 cm-1, which corresponded to the stretching of the O-H bond. At 1600 cm -1, it is possible to see O-H hydrogen bridges bending as a result of the interaction between the fillers and the PVA-Cs matrix. The stretching of the C-O bond at 1000 cm-1 is also visible; this was due to the presence of C-OH groups. This agrees with the mechanical strength results, since samples B11PVA-CS/PPy0.3/PEDOT:PSS0.2/MWCNT0.2 and B12PVA-CS/PPy0.3/PEDOT:PSS0.1 /MWCNT0.1/CB0.1 showed high mechanical strength, which reached up to 40.33 MPa, as shown by the results of the mechanical stress test.

Preprints (www.preprints.org) | NOT PEER-REVIEWED | Posted: 28 January 2021 doi:10.20944/preprints202101.0583.v1

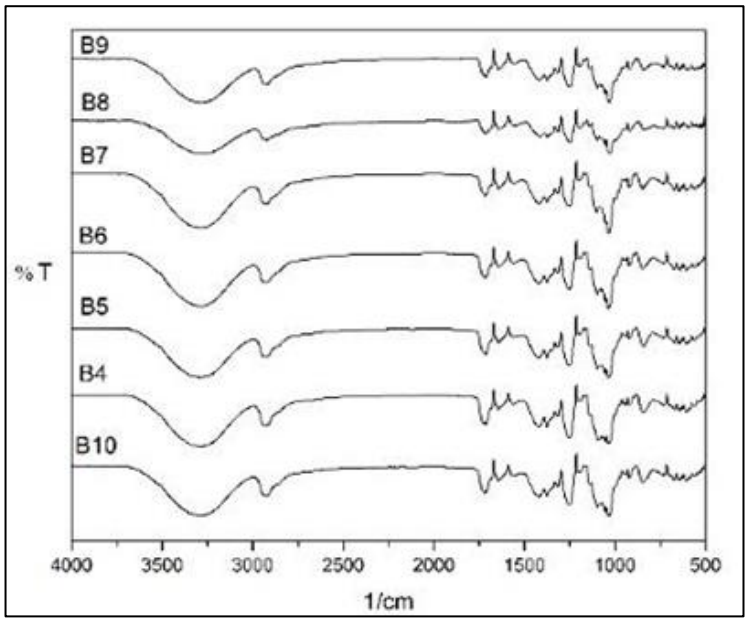

Figure 6. FTIR analysis of the samples B4PVA-Cs/PEDOT:PSS0.2, B5PVA-Cs/PEDOT:PSS0.1, B6PVA-Cs/MWCNT0.2, B7PVA-Cs/MWCNT0.1, B8PVA-Cs/CB0.2, B9PVA-Cs/CB0.1 and B10PVA-Cs.

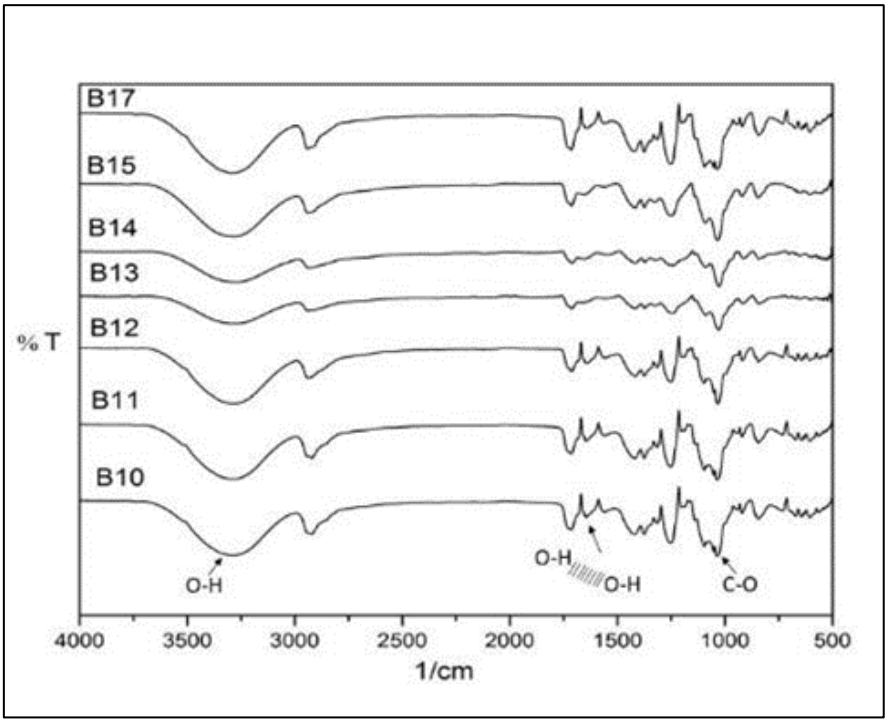

Figure 7. FTIR analysis of samples B10PVA-Cs, B11PVA-CS/PPy0.3/PEDOT:PSS0.2/MWCNT0.2, B12PVA-CS/PPy0.3/PEDOT:PSS0.1 //MWCNT0.1/CB0.1, B13PVA-CS/PPy0.2/PEDOT:PSS0.2/MWCNT0.2, B14PVA-CS/PPy0.2/PEDOT:PSS0.1//MWCNT0.1/CB0.1, B15PVA-CS/PPy0.1/PEDOT:PSS0.2/MWCNT0.2.

3.5 Electrochemical Impedance Spectroscopy (EIS)

The impedance spectra obtained by Electrochemical Impedance Spectroscopy were plotted as a Nyquist diagram and modeled by equivalent circuits.

Figure 8 shows in A) the equivalent circuit for the impedance spectrum of the B1 and B16 samples. This circuit comprises a load Q1 in series, with a load transfer resistance R1, followed by load transfer resistance R2 in parallel with load Q2. This behavior is associated with the ability to transfer load.

Preprints (www.preprints.org) | NOT PEER-REVIEWED | Posted: 28 January 2021 doi:10.20944/preprints202101.0583.v1

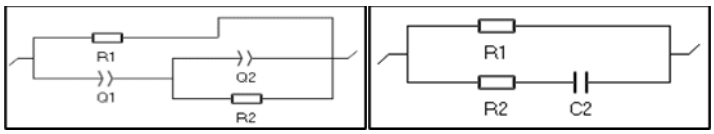

Figure 8. Equivalent circuit a) R1/(Q1+Q2/R2) and b) Equivalent circuit R1/(R2 + C2)

Figure 9 shows the equivalent circuit for the other samples. This circuit comprises two load transfer resistances R1 and R2 in series followed by a capacitance C2. Figure 10 shows the spectra for the PVA-Cs sample. It can be seen in 10(A) that there is a small decrease in the intersection with the semicircle, followed by a line; this effect is due to the transfer of electrons, while the line may be due to the limited diffusion process. In 10 (B), it is possible to see a Bode diagram of magnitude (IZI) and frequency (Hz); the magnitude starts at approximately 4x106 ohm at low frequencies, while at high frequencies the magnitude decreases to 5x105 ohm. Regarding the phase angle, an angle close to -10º can be observed at the beginning in the low frequency region; the phase angle then decreases until reaching -80º. This is because PVA reduces resistive behavior, which results in the predominance of capacitive behavior.

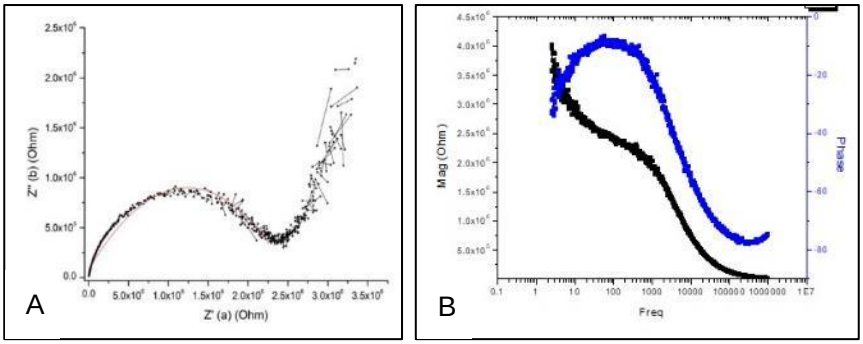

Figure 11. Diagrams of A) Nyquist and B) Bode for the B1PVA-CS/PPy0.3 sample.

Figure 11 shows the diagrams for the B1 sample. Compared with the PVA-Cs sample, 11 (A) shows the presence of a semicircle but at a lower frequency, indicating a transfer of electrons. This is followed by a line that could indicate energy release, since the molecular structure of PPy has double bonds (C=C) alternating with C-C bonds, forming conjugated structures along the chain that allow the transfer of electrons.

The Bode diagram 11(B) of magnitude (IZI) and frequency (Hz) shows that, at lower frequencies, the magnitude starts at approximately 1.3x106 ohm while at high frequencies it reaches almost 0 ohm and remains constant. In the Bode diagram of phase angle (θ) and frequency (Hz), the sample behaves differently because there is an angle offset at lower frequencies; the angle starts at approximately -20º and decreases to -100º. The angle offset can be attributed to the formation of PPy aggregates in the composite material. The opposite occurs at high frequencies; the phase angle starts at -100° and increases up to -55º, which can attributed to the presence of amino (-NH2) groups in Cs and PPy that can be protonated by the -OH groups in the PVA, thus acquiring a positive charge.

Preprints (www.preprints.org) | NOT PEER-REVIEWED | Posted: 28 January 2021 doi:10.20944/preprints202101.0583.v1

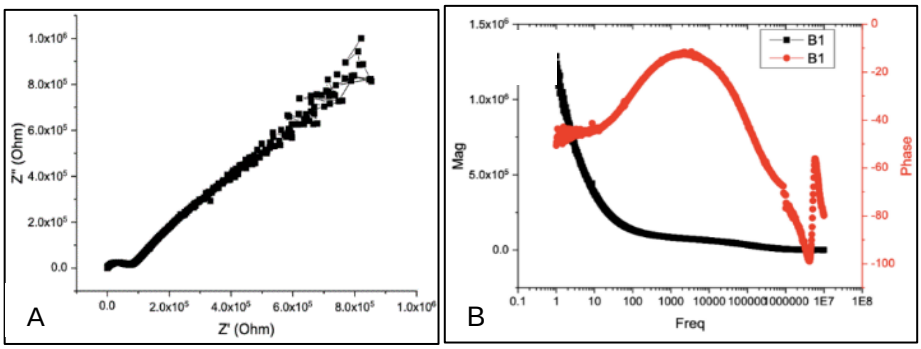

Figure 12 shows the diagrams for the B11PVA-CS/PPy0.3/PEDOT:PSS0.2/MWCNT0.2 sample.

The Nyquist diagram in 12 (A) shows a semicircle indicating load transfer, followed by a pseudo-line indicating energy release. The Bode diagram of magnitude (IZI) and frequency (Hz) in 12 (B) shows an initial magnitude of 4x104 ohm that decreases to 0 ohm and then remains constant. At lower frequencies, the phase angle remains constant at -70º but increases up to 20º at high frequencies it. The sample has a resistive behavior due to the presence of amino groups in the molecular structure of Cs and PPy, which generate a positive charge. PEDOT also contributes to the resistive behavior; it is considered an electroactive polymer due to the presence of interlocking polymer chains that allow the passage of cathodic charges.

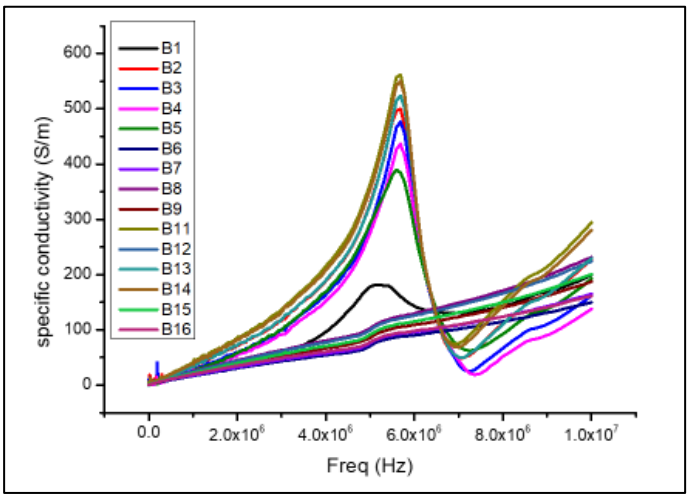

Figure 13. Plot of the conductivities of the samples.

5. Conclusions

The present work is a study of the physical and chemical properties of conductive composite films made from PVA-Cs and 4 fillers (PPy, PEDOT:PSS, MWCNT and CB). The results showed that the incorporation of PPy improved the mechanical properties and Young's modulus of the materials. The analysis of the contact angle showed that all the samples, having an angle of less than 90°, had hydrophilic characteristics, but the samples containing the four fillers showed an increase in their hydrophobic character. It is important to point out that the morphological analysis (SEM) showed that the materials obtained are homogeneous, with no phase separation, which promoted the interaction between the fillers, as demonstrated by the FTIR analysis, which showed evidence of hydrogen bridges in the quaternary samples (those containing the four fillers). One of the most interesting results concerned the interaction between Cs and PVA. The literature reports that Cs improves the mechanical properties of PVA, that is, it increases its Young's modulus. Indeed, in the present work Cs improved the mechanical properties of PVA, but the

best mechanical properties were observed in in the B12PVA-CS/PPy0.3/PEDOT:PSS0.1 //MWCNT0.1/CB0.1 sample, a PVA-Cs material mixed with the four fillers under study. This mixture was made of PVA-Cs/PPy 0.3 g/PEDOT 0.1 g/CNT 0.1 g/CB 0.1 g, and it achieved a Young's modulus of 17.743 MPa , a maximum tensile strength of 40.332 MPa and a deformation of 355.252%, compared to the B10PVA-Cs sample, which had a Young's modulus of 10.858 MPa, a maximum tensile strength of 18.481 MPa and a deformation of 281.932%.

The Nyquist diagram generated with the data from electrical tests showed that the materials containing the fillers under study had decreased resistance due to the transfer of the electrons and the dispersion of the fillers. The Bode diagram showed a different behavior; the samples with higher concentrations of PPy and and PEDOT:PSS at higher concentration showed resistive behavior due to the presence of amino groups in Pp and Cs that interact with the free links of PVA and PEDOT to form a more conductive material . The results of the present work provide important information about the possibility of obtaining composite materials with potential applications in microelectronics.

References

1. Krukiewicz, K., Chudy, M., Vallejo-Giraldo, C., Skorupa, M., Więcławska, D., Turczyn, R., & Biggs, M.. Fractal form PEDOT/Au assemblies as thin-film neural interface materials. Biomedical Materials, **2018**, 13(5), 054102. doi: 10.1088/1748-605x/aabced.
2. Tummalapalli, M., Berthet, M., Verrier, B., Deopura, B., Alam, M., & Gupta, B. Composite wound dressings of pectin and gelatin with aloe vera and curcumin as bioactive agents. International Journal Of Biological Macromolecules, **2016**, 82, 104-113. https://doi.org/10.1016/j.ijbiomac.2015.10.087
3. Huang, Y., Kormakov S., He, X., Gao, X., Zheng, X., Liu, Y., Sun, J., Wu, D., Conductive Polymer Composites from Renewable Resources: An Overview of Preparation, Properties, and Applications, Polymers, **2019**, Vol. 11, No. 187. https://doi.org/10.3390/polym11020187
4. AgilAbraham, Soloman, P., Rejini, V., Preparation of chitosan-Polyvinyl alcohol blends and studies on thermal and mechanical properties, Procedia Technology, **2016**, No. 24, Pag 741-748. https://doi.org/10.1016/j.protcy.2016.05.206
5. Argüelles W., Lizardi, J., Fernandez, D., Recillas, M., Montiel, M., Chitosan Derivates: Introducing Next Functionalities with a Controlled Molecular Architecture for Innovative Materials, Polymers, **2018**, Vol. 10, No. 342. doi: 10.3390/polym10030342
6. Bano, I., Arshad, M., Yasin, T., Afzal, M., Preparation, characterization, and evaluation of glycerol plasticized chitosan/PVA blends for burn wounds, International Journal of Biological Macromolecules, **2019**, No. 124, Pag.155–162. https://doi.org/10.1016/j.ijbiomac.2018.11.073
7. Bourakadi, K., Merghoub, N., Fardioui, M., Mehdi, M., Meftah, I., Essassi, E., Kacem, A., Bouhfid, R., Chitosan/polyvinyl alcohol/thiabendazoluim-montmorillonite bio-nanocomposite films: Mechanical, morphological, and antimicrobial properties, Composites Part B, **2019**, No. 172, Pag. 103-110. https://doi.org/10.1016/j.compositesb.2019.05.042
8. Essel, T., Koomson, A., Seniagya, M., Cobbold, G., Kwofie, S., Asimeng, B., Arthur, P., Awandare, G., Tiburu, E., Chitosan Composites Synthesized Using Acetic Acid and Tetraethylorthosilicate Respond Differently to Methylene Blue Adsorption, Polymers, **2018**, Vol. 10, No. 466. doi: 10.3390/polym10050466
9. García, C., Soltero, F., Bossard, F., Rinaudo, M., Biomaterials Based on Electrospun Chitosan. Relation between Processing Conditions and Mechanical Properties, Polymers, **2018**, Vol.10, No. 257. doi: 10.3390/polym10030257
10. Villemin, E., Lemarque, B., Thiet, T., Quynh, V., Trippé-Allard, G., Martin, P., Lacaze, P., Lacroix, J., Improved adhesion of poly(3,4-ethylenedioxythiophene) (PEDOT) thin film to solid substrates using electrografted promoters and application to efficient nanoplasmonic devices, Synthetic Metals, **2019**, No. 248, Pag. 45–52. doi: 10.1016/j.synthmet.2018.12.010
11. Ko, Y., Kim, J., Kim, D., Kwon, G., Yamauchi, Y., You J., Fabrication of Highly Conductive Porous Cellulose/PEDOT:PSS Nanocomposite Paper via Post-Treatment, Nanomaterials, **2019**, Vol. 9, No. 612. doi: 10.3390/nano9040612.
12. Meng, Q., Jiang Q., Cai, K., Chen, L., Preparation and thermoelectric properties of PEDOT:PSS coated Tenanorod/PEDOT:PSS composite films, Organic Electronics, **2019**, No. 64, Pag. 79–85. https://doi.org/10.1016/j.orgel.2018.10.010
13. Ni, D., Song, H., Chen, Y., Cai, K., Free-standing highly conducting PEDOT films for flexible thermoelectric generator, Energy, **2019**,No.170, Pag. 53-61. https://doi.org/10.1016/j.energy.2018.12.124
14. Popov, A., Brasiunas, B., Mikoliunaite, L., Bagdziunas, G., Ramanavicius, A., Ramanaviciene, A., Comparative study of polyaniline (PANI), poly(3,4-ethylenedioxythiophene) (PEDOT) and PANI-PEDOT films electrochemically deposited on transparent indium thin oxide based electrodes, Polymer, **2019**,No. 172, Pag.133-141. https://doi.org/10.1016/j.polymer.2019.03.059
15. Wang, F., Zhang, X., Ma, Y., Chen, D., Yang, W., Conductive HNTs-PEDOT hybrid preparation and its application in enhancing the dielectric permittivity of HNTs-PEDOT/PVDF composites, Applied Surface Science, **2018**, No. 458, Pag. 924–930. https://doi.org/10.1016/j.apsusc.2018.07.077

16. Zarrin, N., Tavanai, H., Abdolmaleki, A., Bazarganipour, M., Alihosseini, F., An investigation on the fabrication of conductive polyethylene dioxythiophene (PEDOT) nanofibers through electrospinning, Synthetic Metals,**2018**, No. 244, Pag. 143–149. https://doi.org/10.1016/j.synthmet.2018.07.013
17. Guo, X., Bai, N., Tian, Y., Gai, L., Free-standing reduced graphene oxide/polypyrrole films with enhanced electrochemical performance for flexible supercapacitors, Journal of Power Sources, **2018**, No. 408, Pág. 51–57. https://doi.org/10.1016/j.jpowsour.2018.10.083
18. Saugo, M., Flaminil, D., Saidman, S., Formación electroquímica de películas de polipirrol sobre Nitinol a partir de soluciones de ácido sulfosuccínico, Revista Materia,**2018**, Vol. 23, No.2. http://dx.doi.org/10.1590/s1517-707620180002.0391
19. Urper, O., Çakmak, I., Karatepe, N., Fabrication of carbon nanotube transparent conductive films by vacuum filtration method, Materials Letters, **2018**, No. 223, Pag. 210–214. https://doi.org/10.1016/j.matlet.2018.03.184
20. Zhou, H., Zhai, H., A highly flexible solid-state supercapacitor based on the carbon nanotube doped graphene oxide/polypyrrole composites with superior electrochemical performances, Organic Electronics, **2016**, No. 37, Pag. 197-206. https://doi.org/10.1016/j.orgel.2016.06.036
21. Burcu, E., Aydin, M., Kemal, M., Electrochemical immunosensor based on chitosan/conductive carbon black composite modified disposable ITO electrode: An analytical platform for p53 detection, Biosensors and Bioelectronics, **2018**, No. 121, Pag. 80–89. Doi: 10.1016/j.bios.2018.09.008
22. Zhan, P., Zhai, W., Wang, N., Wei, X., Zheng, G., Dai, K., Liu, C., Shen, C., Electrically conductive carbon black/electrospun polyamide 6/poly(vinyl alcohol) composite based strain sensor with ultrahigh sensitivity and favorable repeatability, Materials Letters, **2019**, No. 236, Pag. 60–63. https://doi.org/10.1016/j.matlet.2018.10.068
23. García, C., Soltero, F., Bossard, F., Rinaudo, M., Biomaterials Based on Electrospun Chitosan. Relation between Processing Conditions and Mechanical Properties, Polymers, **2018**, Vol.10, No. 257. doi: 10.3390/polym10030257
24. Islam, Atif & Yasin, Tariq & Akhtar, Muhammad & Imran, Zahid & Sabir, Aneela & Sultan, Misbah & Khan, Shahzad & Jamil, Tahir. Impedance spectroscopy of chitosan/poly(vinyl alcohol) films. Journal of Solid State Electrochemistry, **2016**, 20. 571-578. doi: 10.1007/s10008-015-3082-6